Using ADCP Background Sound Levels to Estimate Wind Speed

by

Len Zedel

Submitted to Journal of Atmospheric and Oceanic Technology

Department of Physics and Physical Oceanography
Memorial University of Newfoundland and Labrador

October 13, 2000

1 Abstract

It is well known that ambient sound is generated by wind through the process of wave breaking and bubble injection. The resulting sound levels are highly correlated with wind speed and, even though the physical process is not fully understood, sound levels can be used to estimate wind speeds with accuracies comparable to other marine wind measurement techniques. It has been noted by several researchers that background sound levels in ADCP system are correlated to wind speeds, however, conventional wisdom would suggest that this signal should be dominated by thermal noise. In this report, background sound levels in 75, 150, and 300 kHz ADCP systems have been investigated. Techniques required to convert raw data into absolute sound levels and to adjust these values to estimate representative surface sound levels are presented. Only the background sound levels in the 150 kHz ADCP retains a signal from the surface generated ambient sound. For these systems, deployment independent wind speed estimates can be made with an accuracy of 1.46 ± 1.5 m s^{-1}: accuracies of -0.12 $\pm$ 1.4 m s^{-1} can be achieved when using deployment specific calibration constants. There is also a wind speed dependent signal in the near surface backscatter levels of the 300 kHz system: a preliminary analysis of this data provided wind speed estimates with an accuracy of -1.31 ± 2.53 m s^{-1}. The source of this signal is not known, but it probably results from subsurface bubbles caused by wave breaking. In the data analyzed, the surface intensity is very sensitive to the depth of the backscatter and the deployment particulars so that any reliable wind speed estimates from this signal would require further investigation.

2 Introduction

2.1 Background

It has been demonstrated that the background "noise" levels in Acoustic Doppler Current Profiler (ADCP) intensity measurements is proportional to wind speed (Visbeck and Fischer 1995). Use of this signal to extract wind speed provides a convenient additional measurement capability of an ADCP. The observation that the noise level in an ADCP is influenced by ocean ambient sound is however inconsistent with the present understanding of ocean ambient sound. In particular, wind generated ambient sound levels decrease at around 19 dB/decade with increasing frequency. Extrapolating observed sound levels to higher frequencies suggests that the thermal noise would mask any wind generated signals at frequencies above 100 kHz. There are however very few observations of ocean ambient sound at high frequencies: the highest frequency observations known by the author are observations up to 75 kHz reported by Zedel et al. (1999) and observations at 50 kHz by Scrimger et al. (1987). It is important to note that the high frequency observations by Zedel et al. are consistent with the -19 dB/decade spectral slope. Wind speed estimates made using 75 kHz sound were however of significantly poorer quality than those made at lower frequencies.

Given the present understanding of wind generated ambient sound, this study has two specific goals. First, to investigate if the behavior of the ADCP noise levels are consistent with wind generated ambient sound. Secondly, to determine the accuracy and consistency of wind speed estimates based on ADCP noise levels.

2.2 Wind Generated Ambient Sound

It has long been known that ambient sound levels in the ocean can be related to surface wind speeds (Knudsen et al. 1948). The ambient sound spectrum is characterized by levels that decrease at a rate of 19 dB/decade with frequency. Sound power levels at 8 kHz range from 35 to 60 dB (re 1 μPa at 1 m depth). The source of this sound is the oscillations of bubbes injected into the ocean as waves break (Medwin and Beaky 1989). The strong correlation of sound levels to wind speed results because the sound energy emitted by a breaking wave is proportional to the energy lost by the wave (Melville et al. 1988).

There have been many reports relating ambient sound levels to wind speed (e.g. Bourassa 1984, Evans et al. 1984, Lemon et al. 1984, Wille and Geyer, 1984, and Vagle et al. 1990). Even though the exact source mechanism is not understood, the existence of a logarithmic relationship between wind speed and sound levels is well established empirically (Evans et al. 1984);

$$log(V) = A \times ssl + B, \tag{1}$$

where V is the wind speed, ssl is the sound level in dB (re $1\mu Pa/\sqrt{Hz}$), and A and B are empirical constants. Equation (1) forms the basis for most estimates of wind speed from ambient sound. Vagle et al. (1990) describe an approach to make the calibration coeficients site independent by accounting for deployment geometry.

2.3 Thermal Noise

The ultimate limit to sound level detection occurs when the pressure fluctuation associated with the sound becomes comparable to the random pressure fluctuations due to the thermal motion of particles in the medium. This limit was first reported by Mellen (1952) who developed a relation for the thermal noise by considering that energy to be distributed evenly over all modes of oscillation:

$$P_n^2 = \frac{4\pi\rho}{C} K(T + 273.15) f^2 \tag{2}$$

where ρ is the density of water, C is the speed of sound in water, $K = 1.38 \times 10^{-23}$ J $^{\circ}$K^{-1} is Boltzman's constant, T is the Celsius temperature, and f is frequency.

The value of P_n^2 does not change much in the ocean because temperature is restricted to the range $0 < T < 35$ $^{\circ}$C and the term $(T + 273.15)$ is constant to within 10%. The dominant term in Equation (2) is the frequency. An example of sound levels in the ocean is shown in Figure 1 along with the theoretical thermal noise limit. The spectra for wind speeds of 4, 10 and 18 m s^{-1} clearly show the characteristic -19 dB/decade spectral slope. A noise floor spectrum was created by taking the minimum spectral level detected for each frequency range over the entire deployment. Also shown in Figure 1 is the theoretical thermal noise level.

The results shown in Fig. 1 are typical of what is expected for ocean ambient sound. At frequencies below 5-6 kHz, low attenuation and high source levels assure that the wind generated spectrum is visible even at low sea states. Above 10 kHz, the observed spectrum begins to flatten out and then at higher frequencies it starts to increase as constrained by the thermal noise level. Notice in particular that if extrapolated, the mean observed sound levels and the thermal noise limit cross at around 100 kHz. Given the data shown in Fig. 1, there is little reason to expect sound levels at above 100 kHz to be representative of surface generated sound and consequently wind speed.

2.4 Field Data

Data from six deployments of ADCP's operating at 75, 150, and 300 kHz have been investigated. The deployment details for each of the data sets is described in Appendix I. In summary: the Sable deployment is a bottom moored 300 kHz ADCP in 19 m of water, the Placentia deployments are two 300 kHz ADCP's positioned at 110 m depth in water of 304 m and 428 m depth, the Faroe Islands deployment is a 75 kHz unit positioned at 825 m depth in 1500 m of water, and the OWS Mike deployments are at 198 m and 124 m depth in approximately 2000 m of water.

2.5 Data Extraction

One of the difficulties in extracting ambient sound levels from ADCP profile data is that of identifying profile segments not contaminated by surface or profile backscatter. To be suitable for extracting ambient sound levels, profile bins representing locations that are in fact located above the surface are ideal. A typically configured ADCP does not normally include more than a couple of

such bins and the surface signature can extend several bins above the surface. In this section, the preliminary data extraction undertaken for the Placentia Bay data sets is presented: data extraction for the other data sets involved the same basic steps with similar results.

A good overview of the ambient sound data quality is achieved by considering a time series of the raw backscatter intensity profiles such as shown in Figure 2 for Placentia Bay deployment P718. The surface is clearly visible at 105 m and there are about 5 additional data bins recorded beyond the surface. By inspecting Figure 2 it is clear that there are times when surface clutter is affecting the last recorded bin: consider the two disturbances at Julian day 115 and 120. In the case of this deployment, the last bin appears to contain uncontaminated data that should represent background noise levels most of the time.

The last intensity bin shown in Figure 2 is extracted and presented as a time series in Figure 3a for both of the Placentia Bay 1999 ADCP deployments; Figure 3b shows the wind speeds recorded at the town of Argentia for the corresponding time interval. Inspection of the data in Figure 3 demonstrates the correlation that has been reported between ADCP noise levels (in this case at 300 kHz) and wind speed. This correlation can be better demonstrated by a scatterplot of noise levels against wind speed as shown in Figure 4a: there is some relationship between wind speed and intensity however there is a great deal of scatter. It must be remembered that for this case the wind speed measurements have been made about 100 km from the ADCP observations separated by a rugged coastline so some irregularity is expected. Notice that in this case, there appears to be a threshold speed somewhere between 5 and 10 $\mathrm{m\,s^{-1}}$.

A second comparison that can be made in the present case is between the raw intensity levels seen in the two ADCP's. It is quite clear from Figure 3a that these two signals are well correlated. Figure 4b shows a scatterplot between intensity levels at mooring P718 and those at P879. Here we see substantially better agreement indicating that there is definitely some consistent signal present in the data. It is however also obvious from Figure 4b and Figure 3a that the signal levels from separate instruments are decidedly different. It is essential that before any attempt is made at comparing these results the data must be calibrated so that meaningful comparisons can be made between deployment locations.

3 Calibration

There are two components to calibrating the ADCP systems to measure absolute ambient sound levels. First, the instrument itself must be calibrated to convert the recorded levels into absolute pressure levels. These measured levels must then be corrected to account for environmental considerations including deployment depth and the wind generated ambient sound directionality so that surface sound levels can be recovered.

3.1 Instrument Calibration

Consider the pressure signal received by the ADCP system to consist of two parts;

$$P^2 = P_n^2 + P_a^2 \tag{3}$$

where P_n^2 is the thermal noise component as given by (2) , and P_a^2 is the wind generated ambient sound signal. It is assumed that all reverberation signal has died away. The ADCP's logarithmic receiver takes the pressure fluctuations detected at the transducer face and converts that to a recorded signal, we can express this conversion as

$$10^{k_c E/10} = \xi(P_n^2/Q_n + P_a^2/Q_a) \tag{4}$$

where E is the intensity counts recorded by the ADCP, k_c is the analog-to-digital conversion calibration factor (typical values for k_c are about 0.45 dB/LSB), ξ is an (unknown) system sensitivity converting pressure to voltage and it accounts for transducer efficiency and any amplifier gain, Q_n is the directivity factor for (omnidirectional) thermal noise, and Q_a is the directivity factor for wind generated ambient sound.

For the omnidirectional thermal noise,

$$Q_n = 4\pi / \int \frac{1}{R^2} \frac{J_1(ka\,sin(\theta))}{ka\,sin(\theta))} ds \simeq (ka)^2, \tag{5}$$

where k is the acoustic wavenumber, a the transducer radius, J_1 is the Bessel function of the first kind, θ is the angle between the transducer axis and the source element ds, and the integral is over a spherical surface of radius R (Clay and Medwin 1977). For the ambient sound component, it is necessary to consider the directionality of the surface sound and the fact that the ADCP transducers are directed obliquely to the surface at some angle $\phi = 20°$ or $30°$ depending on the system orientation. Modifying Equation (5) to account for these changes,

$$Q_a = 4\pi / \int \frac{cos^2(\theta)}{R^2} \frac{J_1(ka\,sin(\theta_\phi))}{ka\,sin(\theta_\phi))} ds \simeq (ka)^2 / cos(\phi), \tag{6}$$

where θ_ϕ is the angle between the beam axis and a vertical at the source location, in this case the integral is over an infinite plane representing the surface.

The only unknown parameters in Equation (4) are the ambient sound levels that we are interested in measuring P_a^2, and the system sensitivity ξ. Following the approach presented by Deines (1999), ξ can be evaluated from data for which $P_a^2 = 0$. For high frequencies, this condition will occur at low wind speeds and all that is required is to find the minimum value of $E = E_0$. Setting $P_a^2 = 0$ and setting $E = E_0$, Equation (4) can be rearranged to find,

$$\xi = \frac{k^2 a^2 C}{4\pi\rho K T f^2} 10^{k_c E_0/10}. \tag{7}$$

Equation (4) can now be rearranged to solve for P_a expressed as a sound level in dB (re. 1 μPa):

$$SL = 20\,log\,\frac{P_a}{10^{-6}} = 10\,log(\frac{Q_a}{\xi} 10^{k_c E/10} - \frac{Q_a}{Q_n} P_n^2) + 120. \tag{8}$$

Equation (8) converts recorded intensity counts (E) to absolute sound levels at the receiver depth. Additional corrections for instrument depth (absorption and multiple reflections), band-averaging of the receiver, and the bubble extinction effect must also be considered so that the surface sound level is given by

$$SSL = SL - 20\ log\,\alpha - 20\,log\,\delta \tag{9}$$

where α is a correction factor for deployment depth, and δ is the bubble extinction coefficient.

3.2 Depth Corrections

The intensity of surface generated sound levels decreases as measurements are made farther from the surface. This decrease is only due to the chemical absorption of sound; spherical spreading does not come into play because the ocean surface acts as an infinite plane source. The attenuation effect is however important especially at the frequencies typical of ADCP operation.

For the case of broad-band ADCP's there is an added complication to the problem of correcting for acoustic absorption: these instruments record sound levels over a large range of frequencies so that it is not obvious that a single center frequency based correction is sufficient. The received signal will in fact be an integration over a finite bandwidth so that the measured signal will vary as:

$$P_a^2 = 1/bw \int_{bw} P^2(f)\,\gamma(f, z/\,cos\,\phi)df \tag{10}$$

where P_a^2 is the ambient sound pressure detected by the instrument, bw is the instrument bandwidth, $P^2(f)$ is the source spectrum level at the ocean surface, $\gamma(f, R)$ is the acoustic absorption for a given frequency and range, z is the instrument depth and ϕ is the instrument beam orientation. If f_0 is the instrument center frequency and a spectral slope of -19 dB/decade is assumed for the ambient sound spectrum,

$$P_a^2 = P_0^2(f_0)\,\alpha = 1/bw \int_{bw} (\frac{f}{f_0})^{2\zeta/20}\,\gamma(f, z/\,cos\,\phi)df, \tag{11}$$

where $P_0^2(f_0)$ is the ambient sound source pressure level at f_0, α is a scaling coefficient for the difference between the center frequency response and the band averaged response and $\zeta = -19$ dB/decade.

The correction factor indicated by Equation (11) was determined for a variety of instrument geometries and it is negligibly different from the center frequency value for most configurations. For example, for a 150 kHz system z = 200 m, $\phi = 30°$ and assuming a 50% bandwidth response Equation (11) gives α = -11.6 dB and the single frequency response at 150 kHz gives α = -11.9 dB.

The difference between the single frequency response and the band averaged response is caused by the differential absorption as a function of frequency. As a result, the largest differences occur when substantial signal attenuation is seen. For the present data sets, the largest difference was seen in the 75 kHz data. For an instrument deployed at 850 m, the single frequency response gives α = -27.8 dB compared to the band averaged response of α = -24.0 dB.

3.3 Bubble Extinction

It has been observed that at high wind speeds, ambient sound levels no longer increase with increasing wind speeds (Farmer and Lemon 1984). A demonstration of this effect can be seen in Figure 1 where the sound levels recorded for 18 $\mathrm{m\,s^{-1}}$ winds are lower than those recorded at 10 $\mathrm{m\,s^{-1}}$ at frequencies above 20 kHz. The cause of this anomalous behavior is the introduction of bubbles in the near-surface zone of the ocean which act to absorb the surface generated wind sound. Crowther et al. (1993) provide an empirical correction factor for this extinction process:

$$\delta = K_\beta(f)U^4 \tag{12}$$

where K_β is an empirically determined, frequency dependent coefficient, and U is the wind speed. The values of K_β published by Crowther et al. (1993) are a maximum at 60 kHz and decrease at both higher and lower frequencies (see Fig. 8). The values of K_β found by Crowther et al. are listed in Table 1.

F (kHz)	10	15	20	30	40	60	80	100	150	200	250
K_β (10^{-6})	2.22	4.54	7.34	12.0	15.0	15.8	15.6	14.3	11.0	8.7	7.1

Table 1: Values of the scaling factor K_β from Equation (12) presented by Crowther et al. (1993).

In order to apply the correction determined by Equation (12) , requires knowledge of the wind speed. And, for the present application, the wind speed is not known *a priori*. This correction is applied employing an iterative approach that involves repeatedly estimating the wind speed from the sound level, correcting the sound level for extinction and then estimating the wind speed again. The wind speed is found when the incremental correction becomes small.

3.4 Bottom Interactions

In deep water it is generally safe to assume that the only source of high frequency ambient sound is the ocean surface. This assumption is however not valid in shallow water where surface generated sound can become trapped as it reflects off the surface and the bottom. Depending on the water depth, acoustic frequency, and bottom and surface scattering properties, substantial enhancement in the sound levels can occur (Zedel et al. 1999). When a correction for this effect is required, it is combined with the depth correction factor α.

4 Data Comparisons

By applying the calibration and environmental corrections that have been identified, it is possible to compare ADCP observations from the various deployment locations and operating frequencies. In this section, analysis from the various deployments is grouped according to the system operating frequency and the presentation is in order of increasing ability to measure wind speeds.

4.1 75 kHz, Faroe Islands Deployments

Data from the Faroe Islands was collected as part of a suite of deep water moorings. In this case, the instrument was located at 825 m depth in 1500 m of water and recorded data in 28, 25 m bins. The profile data does not reach to the surface, however, intensity in the last recorded bin at a depth of about 100 m shows very little signal and appears to be representative of background sound levels.

A scatterplot of corrected sound levels against wind speed is presented in Figure 5. There is clearly no correlation of wind speed and 75 kHz sound levels in this data. The sound levels expected at 75 kHz are between 30 to 40 dB (see Figure 1) while the mean value calculated for this deployment are about 47 dB. At this location, the depth correction term in Equation (9) is 25 dB so that the observed values are essentially representative of the 22 dB thermal noise level. In other words, for this instrument located 825 m below the ocean surface, the attenuation associated with 75 kHz sound propagation is eliminating any meaningful signal. It must be noted that the normal deployment depth for these 75 kHz systems is expected to be quite deep so substantial attenuation of surface generated sound will always be a complication.

4.2 300 kHz, Placentia Bay and Sable Island Deployments

Both the Placentia and Sable deployments are made in shallow water ($\simeq$300 m and 19 m respectively). Even at 300 kHz, bottom interactions are a consideration at the Sable location and a 3 dB correction has been applied to this data. Wind speeds are plotted against calibrated sound levels for these deployments in Figure 6a. Here, a correlation is seen for both deployments although there is a lot of scatter.

At first, the results shown in Fig. 6a appear very encouraging however, at a given wind speed the Sable observations are about 10 dB higher than the Placentia observations. Another problem with this data is that the sound levels (50 - 60 dB re. 1 μPa) are at least 20 dB above the values anticipated for 300 kHz ambient sound. These factors suggest that these data might be contaminated by surface backscatter.

To identify data that might be contaminated, different approaches proved suitable for the two data sets. For the Sable data, only data for which the change in intensity beyond the surface range was less than 1 dB/range cell was accepted. For the Placentia data where there was a good deal of profile data in addition to the return at and beyond the surface, the minimum value for the entire profile was taken as the background noise level. Data selected in this manner are shown in Figure 6b and demonstrate no correlation with wind

speed. It is concluded from this trial that there is no wind speed dependent signal in the background noise levels of 300 kHz ADCP's.

4.3 150 kHz, OWS Mike

The two data sets collected at OWS Mike are the best suited to evaluations of sound levels associated with wind speed because they were collected for this purpose. Data was recored with the Ocean Ambient Sound Instrument System (OASIS) which consits of a 150 kHz ADCP modified to record ambient sound at frequencies from 1-75 kHz (Zedel et al. 1999). For both of these deployments, there are at least 15 (8 m) bins sampled beyond the surface so that the process of extracting accurate background intensity levels is not compromised by surface clutter. In addition to the Doppler data, the OASIS instrument collected ambient sound data which provides additional basis for comparison with the ADCP background levels.

An overview of data from the 1996 deployment is provided in Figure 7 through a scatterplot of observed ambient sound levels at a variety of frequencies against the log of the wind speed. Linear regression fits are indicated by straight lines. In Figure 7 the 7.5 kHz data provides a well defined linear relationship between wind speed and sound levels; this tight correlation provides the basis for the wind speed from ambient sound technique. As the comparisons progress to higher frequencies, the quality of the regression is seen to deteriorate. Notice in particular that at 70 kHz, the sound level response to changes in wind speed has become very flat making any wind speed estimates very inaccurate.

At low wind speeds, the sound level at 70 kHz is corrupted by thermal noise. A progressive response is seen for intermediate wind speeds but as the wind speed increases, the 70 kHz sound level actually starts to decrease. The reason for the reduced response is the bubble extinction effect reported by Farmer and Lemon (1984) and Crowther et al. (1993). At higher wind speeds, breaking waves introduce bubbles into the ocean mixed layer leading to progressively higher extinction effects with increasing sea state. Observations by Crowther et al. (1993) show that this extinction effect is most pronounced at around 60 kHz due to a peak in the concentration and acoustic cross-section of the near surface bubbles. It is very interesting that while the 70 kHz data does not provide a reasonable ambient sound response, the 150 kHz ADCP data again provides a good regression fit.

Another view of this data is provided in Figure 8 where the data has been sorted by wind speed and presented as spectral plots for wind speeds of 4, 8, 12, and 16 $\mathrm{m\,s^{-1}}$ for both the 1996 (•'s) and 1997 (∘'s) OWS Mike deployments. In this representation the consequence of the bubble extinction effect is clearly seen at frequencies of close to 60 kHz as the sound level observations bunch up. As a reference, the attenuation effect predicted by Crowther et al. (1993) is indicated by the +'s in Figure 8 assuming a 15 m $\mathrm{s^{-1}}$ wind (0 dB attenuation is indicated as 65 dB). From the bubble extinction response reported by Crowther et al. (1993), the extinction effects at 150 kHz are comparable to those realized at somewhat less than 30 kHz. If the range in sound levels in the present data is taken as an indication of the extinction effect (a reduced range in observed levels suggesting a greater extinction effect), the extinction at 150 kHz is similar to that at 15 kHz.

5 Wind Speed Prediction

The ultimate goal of the present study is to determine the accuracy with which wind speeds can be estimated using ADCP background sound levels. From the observations presented, it is clear that the only ADCP frequency for which this can be attempted is the 150 kHz system. Lower frequencies (75 kHz) encounter the surface bubble extinction maximum while higher frequencies are limited by thermal noise and acoustic absorption.

The generally accepted form for the relationship between wind speed and ambient sound levels as given by Equation (1) predicts a straight line between sound levels in dB and the logarithm of the wind speed. And, the consistency of this relationship is born out by the straight line fits indicated in Figure 7. The coefficients for these fits as well as those for the 1997 data are shown in Table 2. Linear regressions were restricted to that region of the data where there was no apparent influence of bubble extinction. For the three ambient sound measurements (7.4, 15.4, and 30.1 kHz) the coefficients are consistent. The change in slope makes comparison of the intercepts (B) difficult, but for these three frequencies the values are all comparable. The ambient sound measurement made at 69.1 kHz is inconsistent: the slope is far too high due to the overwhelming effects of bubble extinction at this frequency. Finally, the 150 kHz ADCP data again gives a slope value consistent with the lower frequency ambient sound data. Also notice that the intercept (B) values for the 1997 data are smaller in magnitude than the corresponding 1996 values for all frequencies. The origin for this consistent shift can be seen in Figure 8 in that the 1996 data has lower mean SSL values than the 1997 data.

The coefficients given for the 150 kHz ADCP in 1996 have been used in Equation (1) to estimate wind speeds and the results (for 1996) are shown in Figure 9a where measured wind speeds are indicated in red, and the wind speed estimates are indicated in black. In general, a reasonable agreement is achieved however at times of high wind speed, ambient sound based estimates are low because of the bubble extinction effect (notice the errors that occur during high wind speeds that occur on days 152 and 172). These data can be corrected using Equation (12) and the resulting wind speed estimates are indicated in Figure 9 in blue where it can be seen that the differences during high wind speed events has been somewhat reduced. To assist in evaluating the quality of the estimates, Figure 9b shows a time series of speed difference (estimated wind speed minus true wind speed) in black for the raw estimates, and in blue for the extinction corrected estimates. The mean estimate difference and standard deviation are -0.124 $\pm$ 1.44 $\mathrm{m\,s^{-1}}$ for the raw estimates and 0.202 $\pm$ 1.40 $\mathrm{m\,s^{-1}}$ for the extinction corrected values.

Similar comparisons made for the 1997 calibration results are shown in Figure 10a and b where the same plotting conventions have been used as in Figure 9. The results from the 1997 data are similar to that seen in 1996; there is a tendency for estimates to be low at higher wind speeds (see day 123, 1997) and application of the extinction correction goes some way to making up for this error. For the raw speed estimates, the mean difference (estimate minus true wind speed) is 0.136 $\pm$ 1.58 $\mathrm{m\,s^{-1}}$, and for the corrected estimates, 0.567 $\pm$ 1.64 $\mathrm{m\,s^{-1}}$.

Frequency (kHz)	A (1996) (dB^{-1})	B(1996) -	A (1997) (dB^{-1})	B (1997) -
7.4	0.044±0.002	-1.50±0.13	0.042±0.002	-1.35±0.11
15.4	0.053±0.005	-1.69±0.24	0.0431±0.003	-1.12±0.14
30.1	0.056±0.007	-1.57±0.30	0.047±0.005	-1.18±0.20
69.1	0.119±0.007	-3.49±0.27	0.076±0.005	-1.90±0.20
150	0.036±0.002	-0.30±0.06	0.037±0.001	-.24±0.03

Table 2: Wind speed from ambient sound coefficients as estimated from the OWS Mike 1996 data. A represents the slope and B represents the intercept in Equation (1) . Coefficients are shown for both the 1996 and 1997 OWS Mike deployments.

Good wind speed estimate results are to be expected when the data set for which wind speeds are being estimated is the same data upon which the calibration estimates were based. And, it is clear from Figure 8 that significant differences exist between the 1996 and 1997 deployments. Calibration factors from 1996 can be used on the 1997 data and vice-versa to evaluate accuracy but such conversions results in significant over and under estimates. A more reasonable best estimate for universal calibration constants given the present data sets can be arrived at by taking the average of the two calibration values. Expectations for success in forming such an average is supported by the fact that both A and B values for 1996 and 1997 agree within statistical uncertainty. Averaged values for the calibration constants are $A = 0.036 \pm 0.002$ dB^{-1}, and $B = 0.270 \pm 0.069$, results when these values are used to form wind speed estimates are shown in Figure 11a (for the 1996 data), and 11b (for the 1997 data): only extinction corrected estimates are shown. As expected from the offset between the 1996 and 1997 observations, estimates for the 1996 data tend to be high (the difference, wind speed estimate minus the true wind speed is 1.46 ± 1.5 $m\,s^{-1}$), and for the 1997 data the estimates are low (difference = -0.41 ± 1.5 $m\,s^{-1}$).

6 Discussion

The prediction of wind speeds using the 150 kHz data has been quite

successful; generalized calibration constants give an uncertainty in wind speed estimates of better than 1.46 $\pm$ 1.5 m s^{-1}. However, there remains a significant difference in sound levels between the 1996 and 1997 OWS Mike data. The difference occurs at all frequencies and all wind speeds appearing to be about 2 dB (consider Figure 8). A difference in overall levels might be expected to arise from the depth correction algorithm but that correction is highly frequency dependent and it would have a greater effect at high frequencies. Some sort of instrumentation effect might also be considered however in this case, both the OASIS system ambient sound data and the 150 kHz ADCP data are effected. If we accept the depth correction algorithm as working correctly, then the only explanation for the change in sound levels is a change in the source level. Such a change might be caused by changes in air-sea temperature difference or changes in surfactants that affect surface tension. Whatever the cause, it appears that there may be an irreducible variability in wind generated sound levels of at least 2 dB magnitude based on the present observations.

In Figure 8, the 150 kHz (ADCP) observations made at 4 m s^{-1} stand out in that they appear below the noise threshold. This outcome is possible because the processing approach being used separates the thermal noise component from the wind generated sound (see Equation (3)). By solving for P_a separate from P_n, it is possible to extract ambient noise levels that are substantially below the thermal limit. In support of the success of this approach, notice that the level of the 150 kHz, 4 m s^{-1} data point is in line with the -19 dB/decade slope and the 4 m s^{-1} data seen at lower frequencies. For this processing scheme, the real detection threshold is that level at which there is no longer any difference between the observed sound level and the thermal noise limit. At 150 kHz, the thermal noise level is 28.8 dB, Figure 12 shows how the difference between total sound level and the thermal noise level varies with surface sound level at 150 kHz (here ignoring any attenuation terms). If there were no thermal noise, the plotted difference would follow the straight dashed line shown in Figure 12 and, when the only component of the received sound level is thermal noise, the value of the difference is 0 dB. Given that the sensitivity of the RD Instruments systems is about 0.5 dB as determined by $k_c \simeq 0.5$ in Equation (4) (indicated by the dashed line in Figure 12), surface sound levels of as low as 20 dB can be resolved with this system. Notice that in Figure 7, the minimum values reported for the 150 kHz ADCP are in fact around 20 dB.

Extinction coefficients presented by Crowther et al. (1993) have been used to correct wind speed estimates for attenuation caused by near surface bubbles. This correction factor has little effect at wind speeds below 10 m s^{-1} but due to the U^4 dependence it becomes a critical correction at higher wind speeds. That being noted, it appears that the correction as applied is not always adequate in the present data set: consider the predictions in the corrected data shown in Figures 9 and 10. The fact that these correction seem (at times) to be inadequate would suggest that the actual coefficient values change in space or even over time at a given location.

7 Summary and Conclusions

ADCP data sets ranging in frequencies from 75 kHz to 300 kHz have been

evaluated for the presence of a wind speed dependent signal in the background noise levels. Conventional wisdom suggests that any background sound levels at above 100 kHz should be dominated by thermal noise in the ocean except at high wind speeds. In addition, the occurrence of bubble clouds injected by breaking waves leads to a wind speed dependent acoustic extinction term. Despite these contrary factors, observations have reported a wind speed dependent component in ADCP background noise levels.

It has been found that the 300 kHz data does not contain any wind speed dependent signal in the background noise but there may be a signal in the intensity of the surface return in this data. The occurence of this signal has been reported by Schott (1989) and Visbeck and Fischer (1995) in 150 kHz and 75 kHz systems. Acoustic backscatter from the oceans near surface originates from subsurface bubble clouds associated with wave breaking (Thorpe and Hall 1983, Crawford and Farmer 1987). The many factors that might affect bubble cloud extent make the degree to which surface backscatter might be used to predict wind speeds questionable. However, this signal may be useful to correct the true ambient sound data for the surface bubble extinction effect.

The 75 kHz ADCP data showed no indication of wind speed dependence in the background sound levels. This result comes as no surprise as 75 kHz is close to the frequency of maximum extinction due to surface bubble populations and analysis of 75 kHz ambient sound has also indicated poor correlation with wind speed (Zedel et al. 1999). An additional complicating factor with this data is the fact that the instrument was located some 800 m beneath the surface leading to substantial signal attenuation of any surface generated signal: such attenuation will always be a difficulty with normal deployments of these lower frequency systems.

The 150 kHz data set demonstrated good agreement between background sound levels and the logarithm of the wind speed. It appears that this frequency represents an opportunity in the wind generated ambient sound spectrum located above the bubble extinction peak at 60 kHz and below the thermal noise floor. When this data was calibrated to account for instrument sensitivity and threshold levels and when deployment specific factors had been taken into account, wind speed estimates with an accuracy of better than 0.57 ± 1.64 m s^{-1} were realized. This accuracy degraded to 1.46 ± 1.5 m s^{-1} when using deployment independent scaling coefficients: this is an accuracy that should be achievable for any deployment.

8 Acknowledgement

The data required for this study could not have been acquired without the generous sharing of data from several individuals. I should like to recognise the support of Svein Osterhus of the University of Bergen for assisting with the collection of the OWS Mike data sets and for providing me with the Faroe Islands data. I received the Sable Island data from Mark MacNeil of Coastal Ocean Associates Inc. I should also like to recognize RD Instruments support for this project.

9 References

Bourassa, S. L., 1984: Measurement of oceanic wind speed using acoustic ambient sea noise. Masters thesis, University of Rhode Island, 106 pp.

Clay, C.S., and H. Medwin, 1977: Acoustical Oceanography: Principles and Applications. John Wiley and Sons, New York.

Crawford, G.B., D.M. Farmer, 1987: On the spatial distribution of ocean bubbles. J. Geophys. Res., 92, 8231-8243.

Crowther, P.A., H.J.S. Griffiths, and A. Hansla, 1993: Dependence of sea surface noise in narrow beams on windspeed and vertical angle. in Natural Physical Sources of Underwater Sound, 31-44, Kluwer Academic Press, the Netherlands.

Deines, K.L. 1999: Backscatter estimation using broadband acoustic Doppler current profilers. Proceeding of the IEEE 6'th working conference on Current Measurement, San Diego.

Evans, D. L., D. R. Watts, D. Halpern, and S. Bourassa, 1984: Oceanic winds measured from the sea floor. J. Geophys. Res., 89, 3457-3461.

Farmer, D.M., D. Lemon, 1984: The influence of bubbles on ambient noise in the ocean at high windspeeds. J. Phys. Oceanography, 14, 1762-1778.

Gordon, R.L., L. Zedel, S. Bradley, 1993: National Science Foundation Phase I Final Report; OASIS (Ocean Ambient Sound Instrument System), Report to the National Science Foundation, Award Number III-9260579.

Knudsen, V.O., R. S. Alford, J.W. Emling, 1948: Underwater ambient noise, J. Mar. Res., 22, 410-429.

Lemon, D., D. Farmer, D. Watts, 1984: Acoustic measurements of wind speed and precipitation over a continental shelf. J. Geophys. Res., 89, 3462-3472.

Medwin, H., M. M. Beaky, 1989: Bubble sources of the Knudsen sea noise spectra, J. Acoustic. Soc., 86, 1124-1130.

Mellen, R.H. 1952: The thermal-noise limit in the detection of underwater acoustic signals, J.A.S.A., 24, 478-480.

Melville, W. K., M. Loewen, F.C. Felizardo, A. T. Jessup, and M.J. Buckingham, 1988: Acoustic and microwave signatures of breaking waves. Nature, 336, 54-59.

Schott, F., 1989: Measuring winds from underneath the ocean surface by upward looking acoustic Doppler current profilers. J.G.R., 94, C6, 8313-8321.

Thorpe, S.A., and A.J. Hall, 1983: The characteristics of bubble clouds, breaking waves, and near-surface currents observed using side-scan sonar. Contin. Shelf Res., 1, 353-384.

Vagle, S., W. Large, D. M. Farmer, 1990: An evaluation of the WOTAN technique of inferring oceanic winds from underwater ambient sound. J. Atmos. and Oceanic Tech., 7, 576-595.

Visbeck, M. and J. Fischer, 1995: Sea surface conditions remotely sensed by upward-looking ADCPs. J. Atmos. and Oceanic Tech., 12, 141-149.

Wille, P.C. and D. Geyer, 1984: Measurements on the origin of the wind-dependent ambient noise variability in shallow water, J. Acoust. Soc. Am. 75, 173-185.

Zedel, L., L. Gordon, S. Osterhus, 1999: Ocean Ambient Sound Instrument System: Acoustic estimation of wind speed and direction from a sub-surface package. Journal of Atmospheric and Oceanic Technology, 16, 1118-1126.

10 Appendix I

10.1 Sable 1999

This data set consists of a 300 kHz Workhorse system (S/N 268) deployed in 19 m of water off the Nova Scotia coast close to Sable island. The location of the deployment was 43° 55.46' N, 60° 10.75' W from August 1, 1999 until November 10, 1999. The data were collected into 25, 1 m bins with a 3 second sampling interval and averaged into 15 minute ensembles. This record is in fact part of a much longer record going back about 10 years.

Accurate meteorological data for this location was acquired from a weather station that is maintained on Sable Island (climate station 8204700) about 10 km from the ADCP deployment location. Data available from this location includes hourly weather data and of particular importance to the present study, wind speed and direction.

10.2 Placentia 1999

As part of an ongoing study of circulation along the coast of Newfoundland two 300 kHz ADCP's were deployed in Placentia Bay. Workhorse S/N 879 was deployed at 47° 24.56' N, 54° 4.27' W from April 17, 1999 until June 29, 1999. The instrument (with 20° beam angle) was deployed at 110 m depth in 304 m of water. The system was configured with 29, 4 m bins with a 17 s ping interval collected into 20 minute ensembles. Workhorse S/N 718 was deployed with the same configuration and at the same depth as Workhorse 879, but at location 47° 24.63' N, 54° 24.17' W in 428 m of water from April 17, 1999 until June 29, 1999.

Good meteorological data is not available for these moorings. Data was drawn from the weather station located in the town of Argentia about 50 km away from these two instruments.

10.3 Faroe Islands

The data set from the Faroe Islands consists of six separate 75 kHz BB-ADCP deployments made in an area around the Faroe Islands. Unfortunately, of these six deployments, preliminary surveys of the data and deployment particulars eliminated all but one of the deployments as having potential for the OASIS application. The one deployment retained is identified as FB9706 and represents data recorded at 61° 24.98' N, 8° 17.0' W in 825 m of water. The instrument was deployed upward looking at 825 m depth from June 16, 1997 until June 14, 1998 data were collected in 28, 25 m bins, one profile every 20 minutes. Data from this instrument does not reach the surface.

There is no convenient meteorological station close to the deployment positions of the Faroe Islands deployments. Data could be extracted from the Faroe Islands but the distance and difficulty with topographic effects makes that option undesirable. Wind data for this area was recovered from the Canadian Atmospheric Environment Service weather forecast model. This model produces wind fields every 6 hours. For the present application, model results from 60.63° N, 5.0 ° W was used.

10.4 Ocean Weather Station Mike

Data from Ocean Weather Station (OWS) Mike was collected as part of the OASIS program and as a result it is well suited to the present study. These deployments were made at 66° N, 2° E in approximately 2000 m of water. A 150 kHz upward looking ADCP was deployed at this location from May 15, 1996 until June 23, 1996 at a depth of 198 m and from April 21, 1997 until July 4, 1997 at a depth of 124 m. For both deployment, the profiler was configured to collect data in 40, 8 m bins providing a profile range of 320 m. For this 150 kHz instrument positioned at below 200 m depth this configuration assured many profile bins recorded after the surface echo had been received. In 1996 the data was sampled every 3 minutes based on a 3 ping ensemble while in 1997, the data was sampled every hour based on 20 ping ensembles.

Accurate weather data for this location are available from the OWS Mike station.

Figures

Figure 1

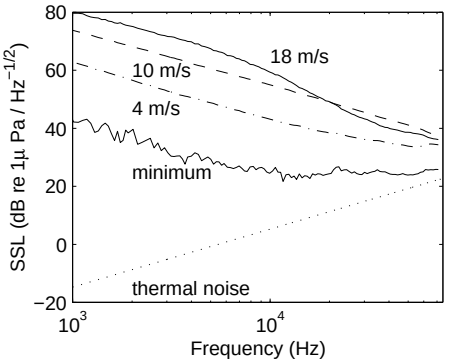

Figure 1: Observations of ocean noise levels from the OASIS instrument for wind speeds of 4, 10, and 18 $\mathrm{m\,s^{-1}}$. The minimum spectral level observed over the entire deployment is also identified as well as the theoretical (omnidirectional) thermal noise limit.

Figure 2

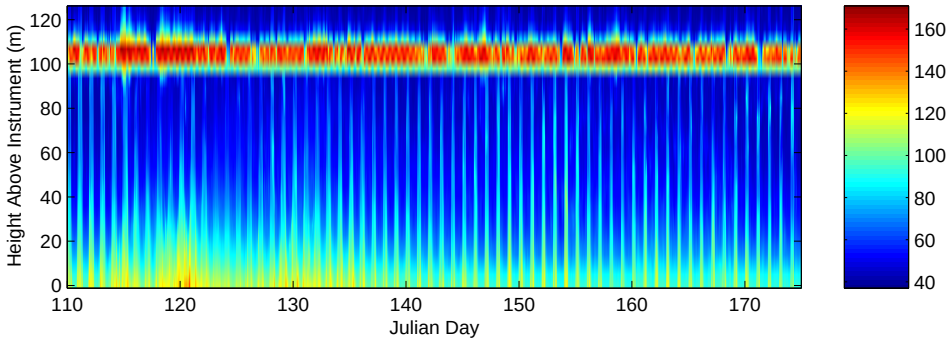

Figure 2: Backscatter intensity recorded from the 70 day Placentia Bay deployment P718. The surface is shown at a height above the instrument of 105 m.

Figure 3

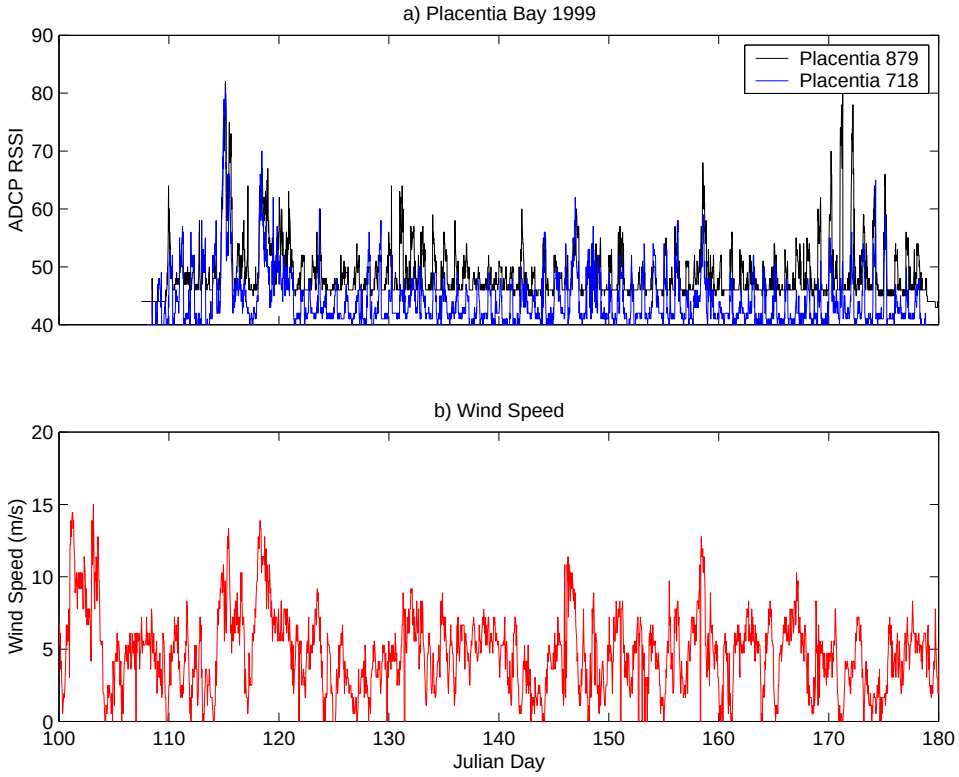

Figure 3: a) Time series of recorded intensity for both Placentia Bay ADCP data sets; averaged levels are displayed for every 20 minutes. b) Wind speed measurements made at the town of Argentia.

Figure 4

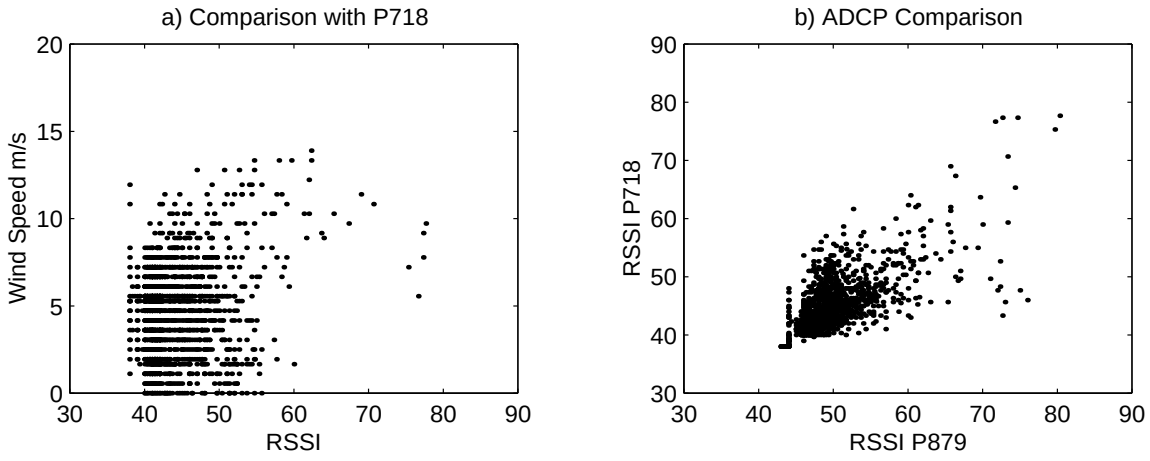

Figure 4: a) Scatterplot between wind speeds observed at the town of Argentia and intensity levels observed at mooring P718. b) Scatterplot between intensity levels observed at mooring P718 and those at P879. Each point represent a one hour average.

Figure 5

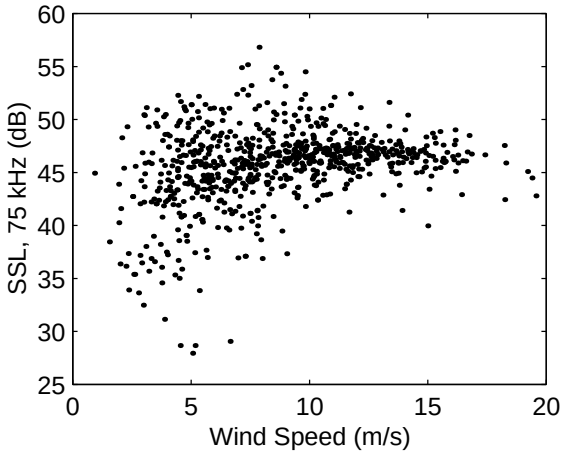

Figure 5: Scatterplot of mooring FB9706, 75 kHz ADCP background sound levels against wind speed. The ADCP was located at a depth of 825 m. Each data point represent 12 hours of data.

Figure 6

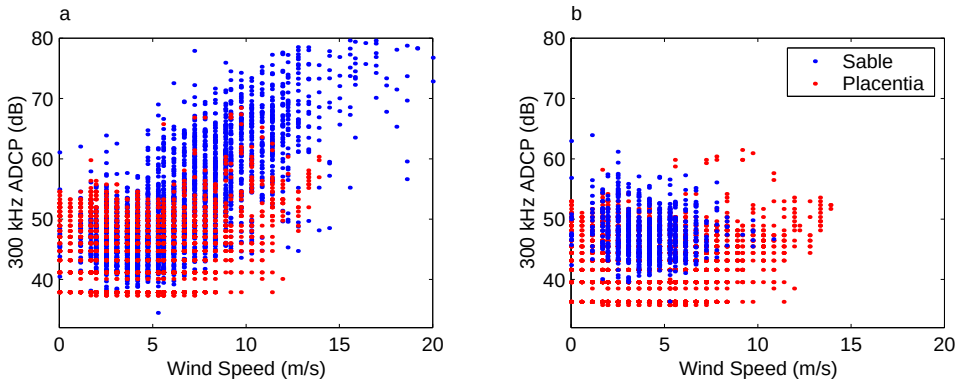

Figure 6: Wind speed, depth corrected 300 kHz ambient sound levels (in dB re 1 μPa Hz^{-1}) scatterplot for the Sable data (blue), and Placentia (red). a) includes all data, b), has been selected to eliminate surface contamination. Each data point represents one hour of data.

Figure 7

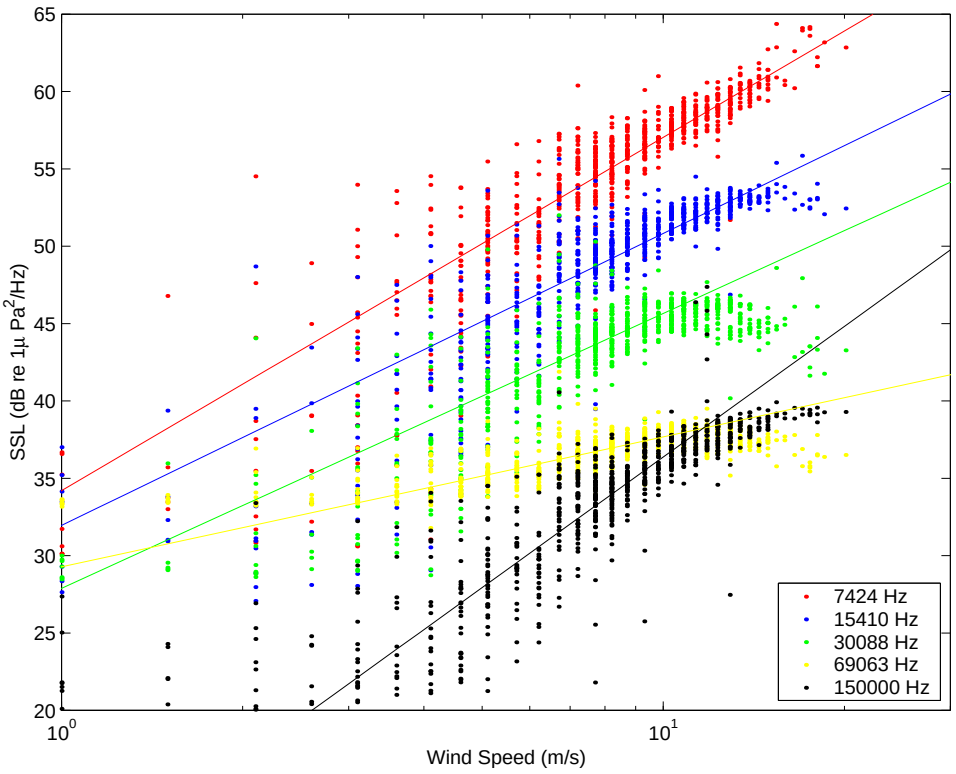

Figure 7: Scatterplot of corrected SSL against log wind speed for 7.5 kHz, 15 kHz, 30 kHz, and 70 kHz OASIS measured ambient sound levels and background sound levels in the 150 kHz ADCP. Based on data from the 1996 OWS Mike deployment. Straight lines represent regression fits to data. Each data point represent one hour of data.

Figure 8

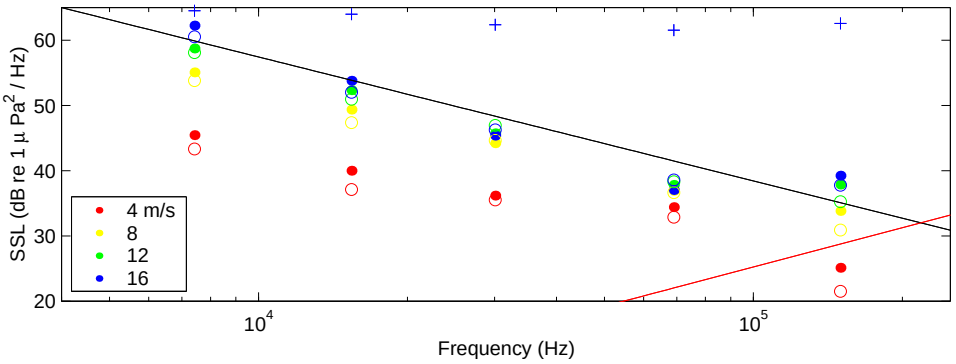

Figure 8: Observed (mean) ambient sound levels at different frequencies for wind speeds of 4, 8, 12 and 16 $\mathrm{m\,s^{-1}}$. The solid black line indicates a -19 dB/decade slope and the solid red line indicates the expected thermal noise limit. Blue +'s indicate the attenuation predicted for the bubble extinction effect by Crowther et al. (1993) at a wind speed of 15 $\mathrm{m\,s^{-1}}$; attenuation is indicated in dB below the 65 dB level with a 0 dB attenuation shown as 65 dB. Results from the OWS Mike 1996 deployment are indicated by •'s, and the 1997 deployments are indicated by ○'s.

Figure 9

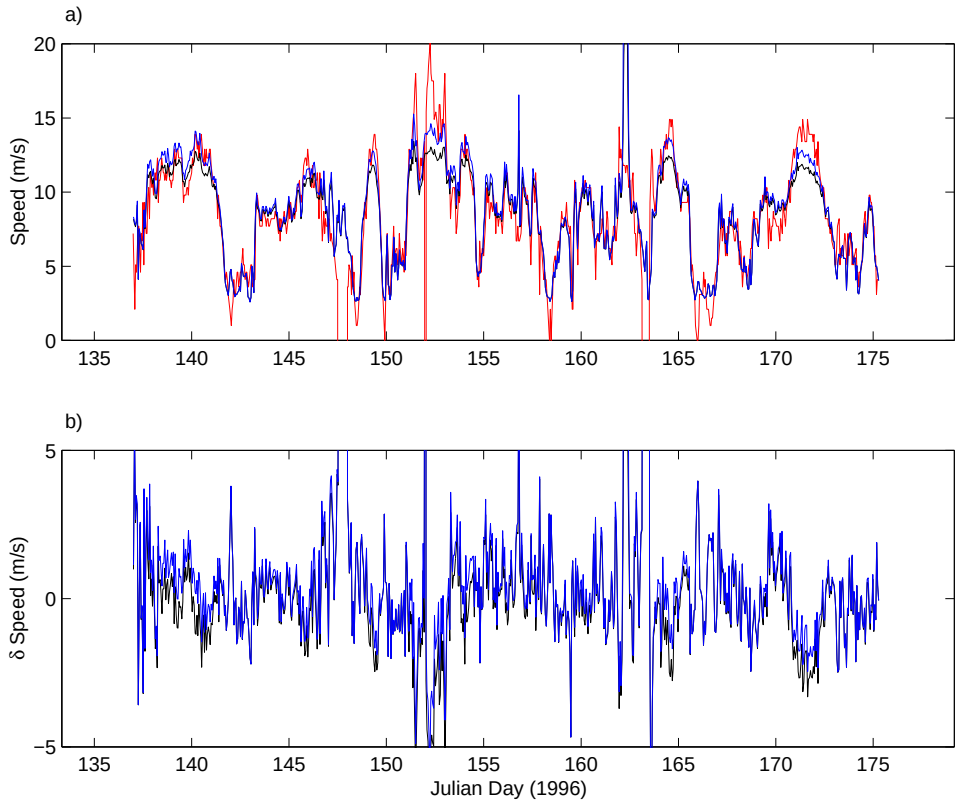

Figure 9: a) Time series of wind speed (red), ADCP based speed estimates (black), and extinction corrected estimates (blue) for the 1996 OWS Mike deployments. b) Difference (speed estimate minus true wind speed) for raw wind speed estimates (black), and extinction corrected estimates (blue).

Figure 10

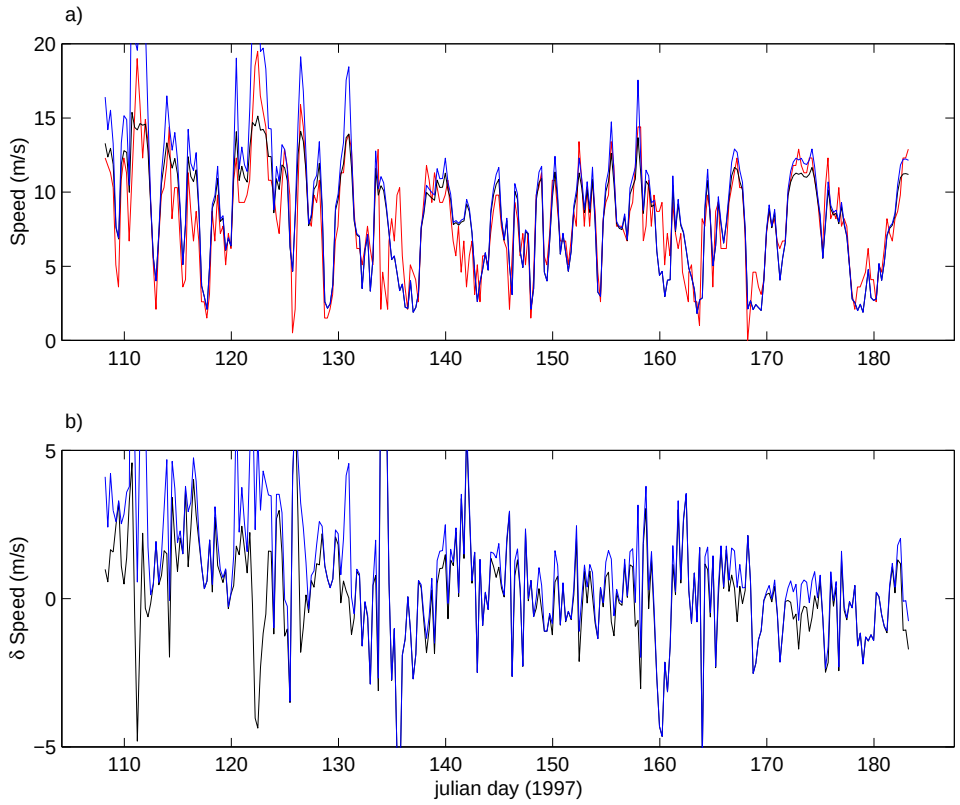

Figure 10: a) Time series of wind speed (red), ADCP based speed estimates (black), and extinction corrected estimates (blue) for the 1997 OWS Mike deployments. b) Difference (speed estimate minus true wind speed) for raw wind speed estimates (black), and extinction corrected estimates (blue).

Figure 11

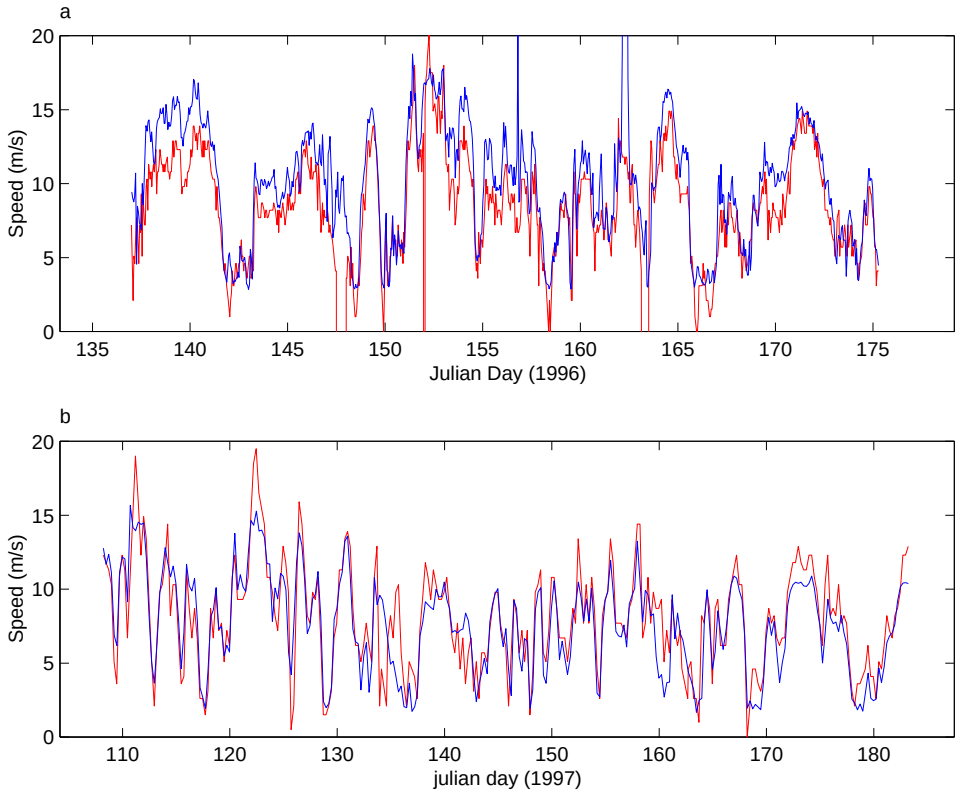

Figure 11: Wind speed estimates for a) the OWS Mike 1996 deployment and b) the 1997 deployment. Estimates shown are based on the averaged calibration constants from 1996 and 1997 and have been corrected for bubble extinction effects.

Figure 12

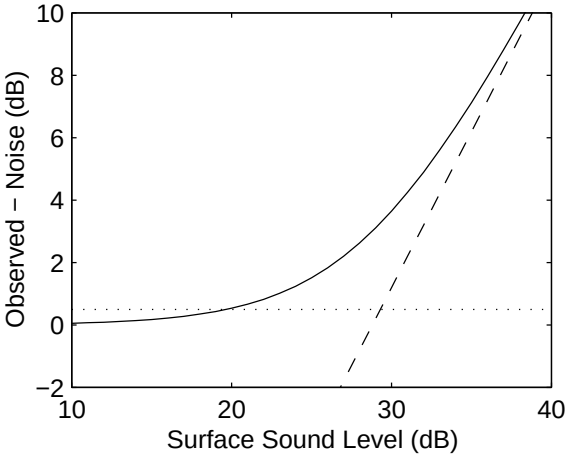

Figure 12: Difference between total sound level and the thermal noise level plotted against surface sound level at 150 kHz ignoring any attenuation terms. The dashed line indicates the ideal result if there were no thermal noise, and the dotted line indicates the 0.5 dB detection limit of the ADCP.